HHS Public Access

Author manuscript

Anal Chem. Author manuscript; available in PMC 2016 October 16.

Published in final edited form as:

Anal Chem. 2015 November 3; 87(21): 11143–11149. doi:10.1021/acs.analchem.5b03350.

Selective detection of protein homologues in serum using an OmpG nanopore

Monifa A. Fahie[‡], **Bib Yang**[†], **Martin Mullis**[†,§], **Matthew A. Holden**[‡,†], and **Min Chen**[‡,†,*]

[‡]Molecular and Cellular Biology Program, University of Massachusetts Amherst, Amherst, Massachusetts 01003

[†]Department of Chemistry, University of Massachusetts Amherst, Amherst, Massachusetts 01003

Abstract

Outer membrane protein G is a monomeric β-barrel porin that has seven flexible loops on its extracellular side. Conformational changes of these labile loops induce gating spikes in current recordings that we exploited as the prime sensing element for protein detection. The gating characteristics - open probability, frequency and current decrease - provide rich information for analyte identification. Here, we show that two antibiotin antibodies each induced a distinct gating pattern, which allowed them to be readily detected and simultaneously discriminated by a single OmpG nanopore in the presence of fetal bovine serum. Our results demonstrate the feasibility of directly profiling proteins in real-world samples with minimal or no sample pretreatment.

Nanopore sensing is a single molecule technique that measures the ionic current flowing through a nanoscopic pore in a membrane[1–3]. Analytes are detected when they cause transient current blockades as they bind or translocate through the pore. The intensity and duration of the blockades provide information about the structure, size and dynamic properties of analytes while the frequency of the blocking events indicates the concentration. Nanopores have been used to detect a large variety of analytes[4], ranging from small molecules, e.g. metal ions[5], organic chemicals[6, 7] and large biological macromolecules, including nucleic acids[8–11] and proteins.[12] For protein sensing, nanopores are usually coupled with a binding site for target proteins to ensure specific detection. The high affinity binding sites used so far have been derived from ligands,[13, 14] inhibitors,[15] peptide sequences,[16, 17] antibodies[18] and aptamers.[19–21] These binding sites are either introduced inside of the nanopore,[18, 21] located at the entrance,[17, 19, 20] or conjugated with an auxiliary polymer in the solution.[13, 22–24] In the latter case, detection is achieved when an analyte binds to a ligand at a polymer and alters the characteristic ionic current signatures derived from the polymer translocation through the nanopore.[22, 23]

[*]Corresponding Author: mchen1@chem.umass.edu. Phone: (413)545 0683.

[§]**Present Addresses**

Molecular and Computational Biology program, University of Southern California, Los Angeles, CA 90089-0371

Supporting Information

Full documentation of material and detailed data analysis are available free of charge via the Internet at http://pubs.acs.org.

Outer membrane protein G (OmpG) is a 14 stranded β-barrel protein derived from *Escherichia coli* (*E. coli*).[25–27] Compared to other well studied protein nanopores, e.g. αHL[28] and MspA[9, 29] that are rigid, oligomeric membrane protein channels, OmpG is a monomeric protein with seven long flexible loops decorated at the extracellular entrance (Fig. 1)[30]. Loop 6 is the most flexible loop, causing the OmpG protein pore to oscillate between the open and closed states.[25, 31–33] As a result, OmpG exhibits frequent gating in current recordings (Fig. 1). Although pores exhibiting continuous nongating conductance have been considered a necessity for nanopore sensing, the gating noise/pattern of OmpG has been exploited as a sensing element for protein detection.[34, 35] In OmpG sensing, analyte binding induces not only a current decrease by obstructing the pore entrance, but also a significant change in gating patterns by altering the dynamic movement of loop 6.[34] The gating pattern is sensitive to the interface formed between OmpG and analyte proteins.[35] Characteristics of gating, such as open probability, gating frequency, event duration and inter-event duration of the gating events provide multiple parameters for analyte identification. Using this strategy, multiple analytes were identified and simultaneously discriminated using a single OmpG nanopore in buffered solutions.[34]

One of the main challenges of protein sensing using nanopores is to identify target proteins in a complex mixture.[36] Most experiments have been performed under ideal conditions using only pure analytes in buffers. To apply this technique as a diagnostic tool for medical use, it is necessary to test the applicability of nanopores for detecting target analytes in clinically relevant samples, e.g. serum, urine or saliva. In this work, we show that two antibiotin antibodies can be readily detected and simultaneously discriminated by a single OmpG nanopore in the presence of 10-fold diluted serum. Our results demonstrate the feasibility of directly profiling proteins in real-world samples with minimal or no sample pre-treatments.

EXPERIMENTAL SECTION

Chemicals and reagents

All chemicals were obtained from Fisher Scientific or Boston Bioproducts unless otherwise stated. Chemicals were used without further purification. SB58C mouse monoclonal antibody was obtained from Southern Biotech (Cat# 6406-01) and BTN.4 mouse monoclonal antibody was obtained from Thermo Scientific (Cat# MS-1048-P1). Diphytanoylphosphatidylcholine (DPhPC) lipids were obtained from Avanti Polar Lipids. Teflon film was obtained from Goodfellow. The maleimide-PEG_2-biotin linker was obtained from Thermo Scientific. Octylglucoside (OG) was obtained from Gold Bio-technology. Hexadecane and pentane were obtained from Sigma Aldrich.

OmpG biosensor preparation

OmpG D224C was purified and labeled with maleimide-PEG_2-biotin as previously described.[34, 35] Briefly, OmpG D224C was expressed in BL21 (pLys) *E. coli* as inclusion bodies. The inclusion body pellet was solubilized in 8 M Urea, 50 mM Tris·HCl pH 8, 2 mM DTT for an hour prior to loading onto a HiTrap Q FF (GE Healthcare Life Sciences). OmpG D224C was then eluted with a gradient of 0–500 mM NaCl, 50 mM Tris-HCl, pH 8.0, 8 M

urea and 2 mM DTT over 60 minutes. Purity of OmpG D224C was verified by SDS-PAGE. Prior to labeling, OmpG D224C was desalted in 50 mM HEPES buffer, pH 7.0 and 8 M Urea to remove DTT and adjust the pH. OmpG D224C was then labeled with maleimide-PEG_2-biotin by mixing OmpG and ligand in a 1:10 molar ratio for 2 hours with constant shaking at room temperature. OmpG was desalted once more in 50 mM Tris-HCl buffer, pH 8.0 in 8 M Urea to remove excess chemicals. OmpG was then diluted 1.5 times in refolding buffer 20 mM Tris-HCl, pH 9.0 with 3.25% octylglucoside and incubated for three days at 37 °C. Refolding and labeling efficiency was tested via a gel-shift assay as previously described (Figure S1).[34] OmpG-biotin was stored at −80 °C in 20% glycerol until further use.

Single Channel Recording

Single channel recording was done as previously described.[34] Briefly, a 100 μm diameter aperture on a 25 μm thick Teflon film separating two chambers was painted with 10% hexadecane in pentane. The pentane was allowed to evaporate prior to filling the two chambers with buffer (10 mM sodium phosphate pH 6, 300 mM KCl). The bilayer was formed by adding 15 μL 10 mg/mL DPhPC lipids in pentane on the aqueous surface of each chamber. Once the pentane evaporated, the buffer was pipetted up and down to coat the aperture with lipids. A Ag/AgCl electrode, with the *cis* electrode connected to ground, was immersed in each chamber. OmpG was pipetted into the *cis* chamber and 200 mV was applied to promote pore insertion into the bilayer. Once a pore was inserted, the voltage was decreased to 50 mV. Since OmpG inserts into the bilayer bidirectionally, the pore gating behavior was observed at both positive and negative 50 mV for five minutes to determine pore orientation.[37] All analyte proteins were introduced to the chamber where the OmpG loops are located. Unlabeled OmpG D224C was tested with SB analyte and did not generate a change in gating behavior (Figure S2). The positive potential is defined as the chamber where the loops are facing is positive. All data was acquired at ±50 mV unless otherwise stated. The Axopatch 200B integrating patch clamp amplifier (Axon Instruments) was used to amplify the current and a 2 kHz Bessel filter was applied. Data was digitized with a Digidata 1320A/D board (Axon Instruments) and acquired at a sampling rate of 100 μs.

Analysis of gating characteristics

Gating characteristics used for generating the fingerprint are defined as shown in Figure S3. To calculate the gating characteristics of SB and BT binding 10 events of at least 1 s from three independent traces were analyzed using the single channel search function in Clampfit 10.3. Errors represent the standard deviation from the three independent pores.

RESULTS AND DISCUSSION

Our OmpG nanopore contains a tethered biotin ligand that can extend into the solution by 30 Å (Fig. 1). We first examined whether an OmpG-biotin nanopore could detect an antibiotin monoclone, SB58C (SB). Addition of 1nM SB to the loop-facing chamber induced a significant change in current traces (Figure. 2). At −50 mV, OmpG-biotin nanopore in the SB bound state exhibited the following characteristics: i) the current of the fully open state decreases slightly by 2 pA as shown in the histogram (Figure 2a, b&c); ii) the current traces

displayed gating patterns markedly different from that of the unbound states (Figure 2a, b). Interestingly, the gating pattern of the SB bound state is heterogeneous, i.e. a single SB binding event induced three different current fluctuation patterns which we named types A, B and C (Figure 2d). We categorize the three types of gating patterns by their open-pore current, open probability and gating frequency (Supporting information Table S1). Type A gating shows that the current was almost constant at −18.3 ± 0.8 pA which is 62 % of the fully open state current. Due to the lack of full gating events, the open probability is 1 and the gating frequency is 0 (Fig. 2c,d). Type B binding shows that OmpG stays mostly closed where the open probability reduces from 0.76 ± 0.03 to 0.13 ± 0.04 with a residual current of 2.1 ± 0.5 pA and a lowered gating frequency of 32 ± 4 s^{-1} (Figure 2d). Type C gating shows that the current fluctuates rapidly with a gating frequency of 77 ± 3 s^{-1}, a 13% increase over that of the unbound state (68 ± 5 s^{-1}) and has an open probability of 0.60 ± 0.06. Each single SB binding event contains multiple combinations of these three types of gating (Fig. 2a). This result is interesting as none of the previous biotin-binding protein analytes, including three streptavidin homologues and three biotin antibodies showed such a phenomenon.[34, 35] Because the gating pattern of the analyte bound state is dictated by the interaction between analyte and OmpG surface, this result indicates when SB bound to the tethered ligand, it often altered the way in which it interacted with the OmpG surface. Our previous study demonstrated that electrostatic attractions are the dominant force that triggers the interaction between analyte and the OmpG loops.[35] Consistent with our previous finding, increasing the salt concentration to 1 M KCl in the recording buffer almost abolished the type B and A binding while the type C binding became similar to the unbound state (Figure S4). Here, we speculate that the SB antibody might contain multiple positively charged regions separately located in areas close to the biotin-binding site. Each positive region can form a unique binding interface with the negatively charged OmpG loops which triggers a gating pattern different from each other. The ability to trigger multiple gating signatures within one binding event is a great advantage for analyte identification and reveals the sensitivity of our OmpG sensor to subtle changes in the analyte surface. At +50 mV, we also observed that a single SB induced the three types of gating patterns albeit with slight variations from those at −50 mV. For example, in Type A binding, the open current changes more than at −50 mV, to 54% of the fully open state current (Supporting information Table S1). Type B has essentially no residual current and a gating frequency of 59 ± 10 s^{-1}. Finally, type C gating frequency is 149.5 ± 8.2 s^{-1} (a 38% increase to that of the unbound state) and an open probability of 0.68 ± 0.05 (17% reduction from the unbound state). This observation is consistent with previous finding that the polarity of voltage has a strong influence on the gating characteristics of the analyte bound state. This is due to two factors: i) the polarity of voltage has a strong influence on the gating of OmpG which exhibits asymmetric current gating at positive and negative potential [34] and ii) the voltage could alter the strength of OmpG and analyte interaction through electroosmotic and/or electrophoretic effects. The binding of SB to OmpG-biotin nanopore was specific as no change in behavior occurred with un-biotinylated OmpG D224C (Fig. S2). The SB antibody appeared to have a high affinity for the biotin ligand as the binding events usually lasted for at least 2 min, 30 times longer than that of a monoclonal antibody BTN.4 that was previously tested, which had a dissociation constant of 1.12 ± 0.28 × 10^8 M^{-1}.[34] SB bound for so long that we were not able to calculate the binding kinetics, mainly because the bilayer does not last long to

allow to collect enough (~1000) events for accurate data analysis. The lowest concentration of SB we detected was 15 pM within 60 min indicating the high sensitivity of our approach.

Previously we have demonstrated that the OmpG-biotin nanopore could discriminate among three biotin antibodies in an antibody protein mixture. To use OmpG nanopore in clinical applications, OmpG would need to detect analyte and possibly discriminate among homologous proteins in serum. Therefore, we investigated how the presence of serum affected the gating of the OmpG-biotin nanopore. In the presence of 25% (v/v) serum the bilayer was unstable, thus we lowered the concentration to 10% (v/v). Addition of 10% (v/v) serum to the chamber where the loops were located induced a noisier gating signal in the OmpG nanopore (Fig. 3). The gating frequency almost doubled at −50 mV (Table S2). Also, the inter-event duration is significantly changed from 6.37 ± 1.88 ms to 0.96 ± 0.31 ms, a 6.6-fold reduction. The open probability and event duration were also affected, undergoing a 5% and 61% reduction, respectively (Table S2). At +50 mV, not only was there an increase in gating behavior but also frequent full blockage events were observed. These blockages could last from seconds to minutes if left unperturbed. Unblocking the pore could be achieved by switching the voltage polarity from +50 to −50 mV. The increased gating frequency and the long closures were likely due to the interaction of serum constituents. These included small molecules and proteins that may have been driven by diffusion, electro-osmosis or electrophoresis into the OmpG lumen. Importantly, despite the high protein content in serum, we did not observe any gating pattern changes that were similar to the analyte protein binding, thereby demonstrating the high specificity of OmpG nanopore detection.

Because the serum-induced blockages at +50 mV reduced the fraction of time the nanopore was able to receive an analyte, we focused on testing the discriminatory ability of OmpG-biotin at −50 mV. As shown in Fig 4a, the addition of two monoclonal antibodies SB58C (SB) and BTN.4 (BT) to the recording chamber containing only buffer triggered binding signals with distinct characteristics that can be recognized qualitatively. Both proteins induced a slight decrease in open pore current (Fig. 4b). The SB-type binding exhibits its typical heterogeneous gating signal while the BT-binding triggered a gating pattern containing a partially closed state with a residual current of 6 pA, which is consistent with previous finding when BT was added to the OmpG-biotin alone.[34] Thus, in the absence of FBS, OmpG could discriminate SB from BT by their respective binding signatures (Fig. 4a, b&c). Although a previous study has also shown a protein A coated solid-state nanopore can discriminate IgG species, the detection relied on their difference in dwell times, which differ by an order of magnitude.[18] Although BT and SB possessed markedly different dwell times (Figure S5), differentiation among the two analytes by OmpG was achieved through their characteristic binding signals. Therefore, this detection mechanism would allow the differentiation of different analytes that have similar dwell times, an advantage that is beginning to be seen with other engineered nanopores.[20, 38]

In the presence of 10% (v/v) serum, the current traces of SB and BT bound states were noisier than those without serum (Fig. 4). Nevertheless, individual binding signatures of SB and BT were well-preserved; both analytes still induced a decrease in the open pore current. The heterogenous gating pattern induced by SB was readily visible. Clearly, the different

gating patterns between SB and BT allowed us to resolve between two homologues in serum (Fig. 4). To quantitatively study how serum affected the gating of the analyte-bound state, we calculated five parameters: open probability, gating frequency, event duration, inter-event duration and open pore current in the presence and absence of serum. When BT bound to OmpG-biotin in the presence of serum, the open probability, event duration and open pore current were not significantly different from those in the absence of serum (Table S2). The inter-event duration was decreased by ~1.5 times and the gating frequency increased by 1.3 times. Similar to BT, moderate changes were also observed for SB type C binding characteristic in the presence of FBS. FBS showed little effect on the type A and type B signals probably due to the lack of gating in these two types of signals. In previous studies, we used the relative values of bound and unbound states to create a fingerprint for analyte identification.[34, 35] The gating fingerprint of BT in the presence of serum compared to the absence of serum was different. This altered fingerprint in the presence in serum was due mainly to the non-specific effects of serum molecules on OmpG gating, rather than a direct effect on the antibody-OmpG interaction. Despite the effect of serum, the fingerprints of the two analytes are clearly distinguishable.

Next we analyzed the effect of serum on the kinetics of analyte binding. The association rate constant k_{on} and dissociation rate constant k_{off} of BT were calculated from the τ_{on} and τ_{off}, respectively, in the absence and presence of FBS (Figure S6). The k_{off} value slightly increased in serum from 0.30 ± 0.09 (n=3) to 0.24 ± 0.05 s^{-1}. However, the k_{on} value decreased from 2.27 ± 0.52×10^7 $M^{-1}s^{-1}$ to 0.83 ± 0.18×10^7 $M^{-1}s^{-1}$ by ~3-fold in FBS. The slower k_{on} of BT in the presence of serum could be due to molecular crowding effects in the high concentration of serum proteins that interact non-specifically with BT and slow its diffusion.[39] This result indicates the serum slightly impedes the sensitivity of OmpG, since detection of the same amount of the binding events in buffer would require longer operating time in serum.

Recently several reports have focused on the issue of sensing specific analytes in protein mixtures.[16, 22] Specifically, an engineered phi29 nanopore containing an engineered peptide sequence was shown to detect a target antibody in 1% (v/v) serum.[16] In this study, current blockage histograms of antibody binding in the presence of serum exhibited two slightly overlapping peaks corresponding to the target protein and serum protein, respectively. Because a small portion of serum protein binding events induced current blockades similar to target antibody, detection could be achieved only when the concentration of target protein is significantly above the interfering impurities. Our work shows that the target binding signals are readily distinguishable from that of serum constituents, allowing unambiguous recognition of each target binding events. Moreover, the fact that OmpG could distinguish two homologous analytes in the presence of serum represents an exciting step forward in nanopore sensing. To date, our OmpG-biotin sensor has been able to discriminate among eight analytes: two monoclonal antibodies, two polyclonal antibodies[34] and four avidin glyco-isoforms.[35] To our knowledge, no other nanopore thus far has shown such selectivity towards as many analytes. The flexible structure of OmpG may adopt distinct conformations for each analyte, which serves as the foundation for generating many unique current gating signals. The high selectivity of the OmpG nanopore can be exploited for profiling of protein homologous or post-translationally modified isoforms. The ability to identify cell-specific

isoforms could aid in the discovery of potential therapeutic targets and disease diagnostics.[40, 41] Thus, as a complementary approach to mass spectrometry and protein micro-arrays for proteomic study, our OmpG nanopore sensor provides a powerful detection platform that could deliver rapid readouts with little or no sample preparation.

CONCLUSIONS

In this study, we have shown that the OmpG nanopore is able to simultaneously detect multiple homologous antibody analytes in serum with high specificity and selectivity. Our study demonstrates the feasibility of protein isoforms profiling in a real-world setting.

Supplementary Material

Refer to Web version on PubMed Central for supplementary material.

Acknowledgments

M.F was supported in part by a Fellowship from the University of Massachusetts Amherst as part of the Chemistry-Biology Interface training grant (T32 GM08515).

References

1. Bayley H, Cremer PS. Nature. 2001; 413:226–230. [PubMed: 11557992]
2. Howorka S, Siwy Z. Chem Soc Rev. 2009; 38:2360–2384. [PubMed: 19623355]
3. Bezrukov SM, Vodyanoy I, Parsegian VA. Nature. 1994; 370:279–281. [PubMed: 7518571]
4. Majd S, Yusko EC, Billeh YN, Macrae MX, Yang J, Mayer M. Curr Opin Biotechnol. 2010; 21:439–476. [PubMed: 20561776]
5. Braha O, Gu LQ, Zhou L, Lu X, Cheley S, Bayley H. Nat Biotechnol. 2000; 18:1005–1007. [PubMed: 10973225]
6. Gu LQ, Braha O, Conlan S, Cheley S, Bayley H. Nature. 1999; 398:686–690. [PubMed: 10227291]
7. Wu HC, Bayley H. J Am Chem Soc. 2008; 130:6813–6819. [PubMed: 18444650]
8. Kasianowicz JJ, Brandin E, Branton D, Deamer DW. Proc Natl Acad Sci U S A. 1996; 93:13770–13773. [PubMed: 8943010]
9. Manrao EA, Derrington IM, Laszlo AH, Langford KW, Hopper MK, Gillgren N, Pavlenok M, Niederweis M, Gundlach JH. Nat Biotechnol. 2012; 30:349–353. [PubMed: 22446694]
10. Wanunu M. Phys Life Rev. 2012; 9:125–158. [PubMed: 22658507]
11. Branton D, Deamer DW, Marziali A, Bayley H, Benner SA, Butler T, Di Ventra M, Garaj S, Hibbs A, Huang X, Jovanovich SB, Krstic PS, Lindsay S, Ling XS, Mastrangelo CH, Meller A, Oliver JS, Pershin YV, Ramsey JM, Riehn R, Soni GV, Tabard-Cossa V, Wanunu M, Wiggin M, Schloss JA. Nat Biotechnol. 2008; 26:1146–1153. [PubMed: 18846088]
12. Movileanu L. Trends Biotechnol. 2009; 27:333–341. [PubMed: 19394097]
13. Movileanu L, Howorka S, Braha O, Bayley H. Nat Biotechnol. 2000; 18:1091–1095. [PubMed: 11017049]
14. Yusko EC, Johnson JM, Majd S, Prangkio P, Rollings RC, Li J, Yang J, Mayer M. Nat Nanotechnol. 2011; 6:253–260. [PubMed: 21336266]
15. Xie H, Braha O, Gu LQ, Cheley S, Bayley H. Chem Biol. 2005; 12:109–120. [PubMed: 15664520]
16. Wang S, Haque F, Rychahou PG, Evers BM, Guo P. ACS Nano. 2013; 7:9814–9822. [PubMed: 24152066]
17. Cheley S, Xie H, Bayley H. Chembiochem. 2006; 7:1923–1927. [PubMed: 17068836]
18. Wei R, Gatterdam V, Wieneke R, Tampe R, Rant U. Nat Nanotechnol. 2012; 7:257–263. [PubMed: 22406921]

19. Rotem D, Jayasinghe L, Salichou M, Bayley H. J Am Chem Soc. 2012; 134:2781–2787. [PubMed: 22229655]
20. Soskine M, Biesemans A, Moeyaert B, Cheley S, Bayley H, Maglia G. Nano Lett. 2012; 12:4895–4900. [PubMed: 22849517]
21. Ding S, Gao C, Gu LQ. Anal Chem. 2009; 81:6649–6655. [PubMed: 19627120]
22. Bell NA, Keyser UF. J Am Chem Soc. 2015; 137:2035–2041. [PubMed: 25621373]
23. Plesa C, Ruitenberg JW, Witteveen MJ, Dekker C. Nano Lett. 2015; 15:3153–3158. [PubMed: 25928590]
24. Kasianowicz JJ, Henrickson SE, Weetall HH, Robertson B. Anal Chem. 2001; 73:2268–2272. [PubMed: 11393851]
25. Yildiz O, Vinothkumar KR, Goswami P, Kuhlbrandt W. EMBO J. 2006; 25:3702–3713. [PubMed: 16888630]
26. Liang B, Tamm LK. Proc Natl Acad Sci U S A. 2007; 104:16140–16145. [PubMed: 17911261]
27. Subbarao GV, van den Berg B. J Mol Biol. 2006; 360:750–759. [PubMed: 16797588]
28. Song L, Hobaugh MR, Shustak C, Cheley S, Bayley H, Gouaux JE. Science. 1996; 274:1859–1866. [PubMed: 8943190]
29. Butler TZ, Pavlenok M, Derrington IM, Niederweis M, Gundlach JH. Proc Natl Acad Sci U S A. 2008; 105:20647–20652. [PubMed: 19098105]
30. Conlan S, Zhang Y, Cheley S, Bayley H. Biochemistry. 2000; 39:11845–11854. [PubMed: 11009596]
31. Chen M, Khalid S, Sansom MS, Bayley H. Proc Natl Acad Sci U S A. 2008; 105:6272–6277. [PubMed: 18443290]
32. Zhuang T, Chisholm C, Chen M, Tamm LK. J Am Chem Soc. 2013; 135:15101–15113. [PubMed: 24020969]
33. Zhuang T, Tamm LK. Angew Chem Int Ed Engl. 2014; 53:5897–5902. [PubMed: 24777684]
34. Fahie M, Chisholm C, Chen M. ACS Nano. 2015; 9:1089–1098. [PubMed: 25575121]
35. Fahie MA, Chen M. J Phys Chem B. 2015; 119:10198–10206. [PubMed: 26181080]
36. Howorka S, Siwy ZS. Nat Biotechnol. 2012; 30:506–507. [PubMed: 22678388]
37. Chen M, Li QH, Bayley H. Chembiochem. 2008; 9:3029–3036. [PubMed: 19012294]
38. Nir I, Huttner D, Meller A. Biophys J. 2015; 108:2340–2349. [PubMed: 25954891]
39. Roosen-Runge F, Hennig M, Zhang F, Jacobs RM, Sztucki M, Schober H, Seydel T, Schreiber F. Proc Natl Acad Sci U S A. 2011; 108:11815–11820. [PubMed: 21730176]
40. Nomura DK, Dix MM, Cravatt BF. Nat Rev Cancer. 2010; 10:630–638. [PubMed: 20703252]
41. Zhao J, Patwa TH, Lubman DM, Simeone DM. Curr Opin Mol Ther. 2008; 10:602–610. [PubMed: 19051138]

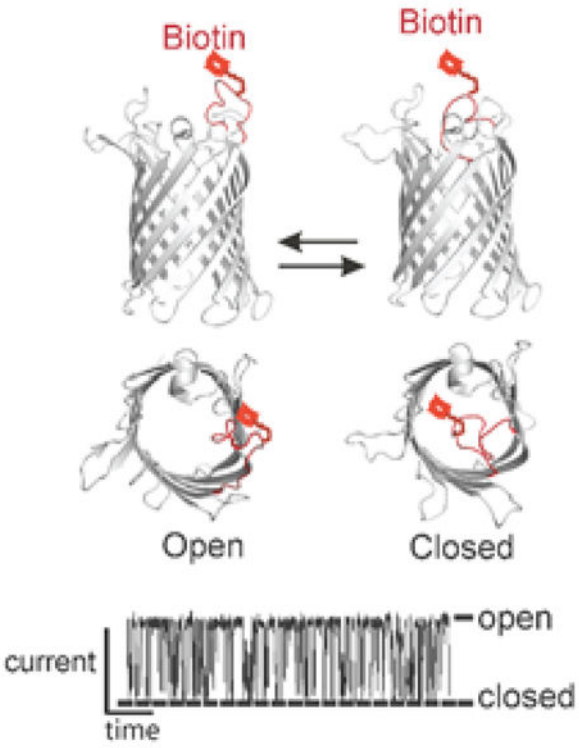

Figure 1.
The open (2IWV) and closed (2IWW) structures of OmpG with the loop 6 highlighted in red. The ionic current trace was obtained in 10mM sodium phosphate pH 6, 300mM KCl buffer.

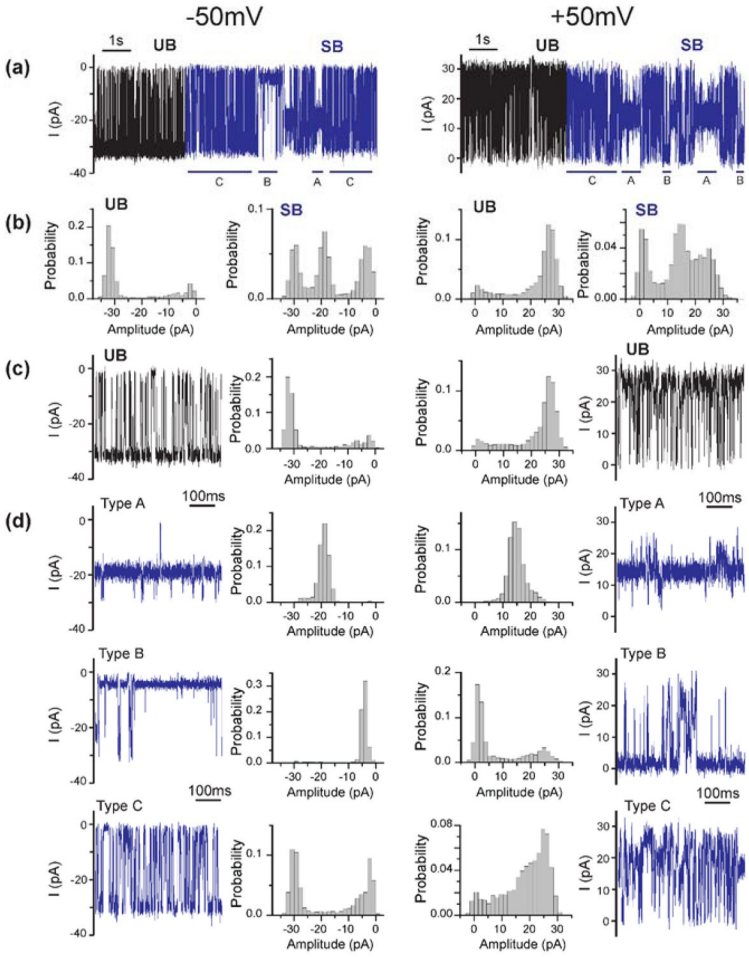

Figure 2.

Detection of SB58C by OmpG-biotin nanopore. (a,b) The electrophysiology traces and all events histograms of unbound (UB) and SB-bound states of OmpG-biotin at −50 mV and +50 mV. (c) Zoomed-in electrophysiology traces and all-events histograms of the unbound state and (d) the three independent SB-binding states types A, B and C. Buffer used was 10 mM sodium phosphate pH 6, 300 mM KCl. 1nM SB antibody was added to the recording chamber. SB binding was recorded with a 2 kHz Bessel filter at a sampling rate of 100 μs.

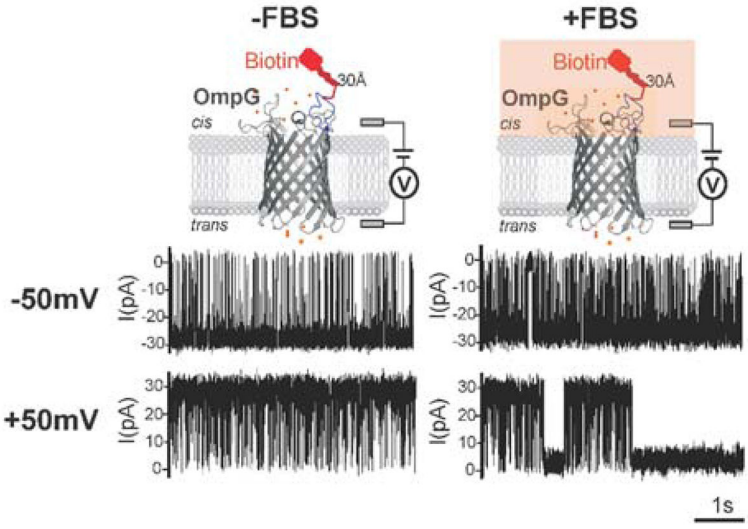

Figure 3.

The effect of serum on the gating behavior of OmpG-biotin. 100 μl of FBS was added to the loop-containing chamber to a final concentration of 10% (v/v). The buffer was 10 mM sodium phosphate pH 6.0, 300 mM KCl. OmpG was recorded with a 2 kHz Bessel filter at a sampling rate of 100 μs.

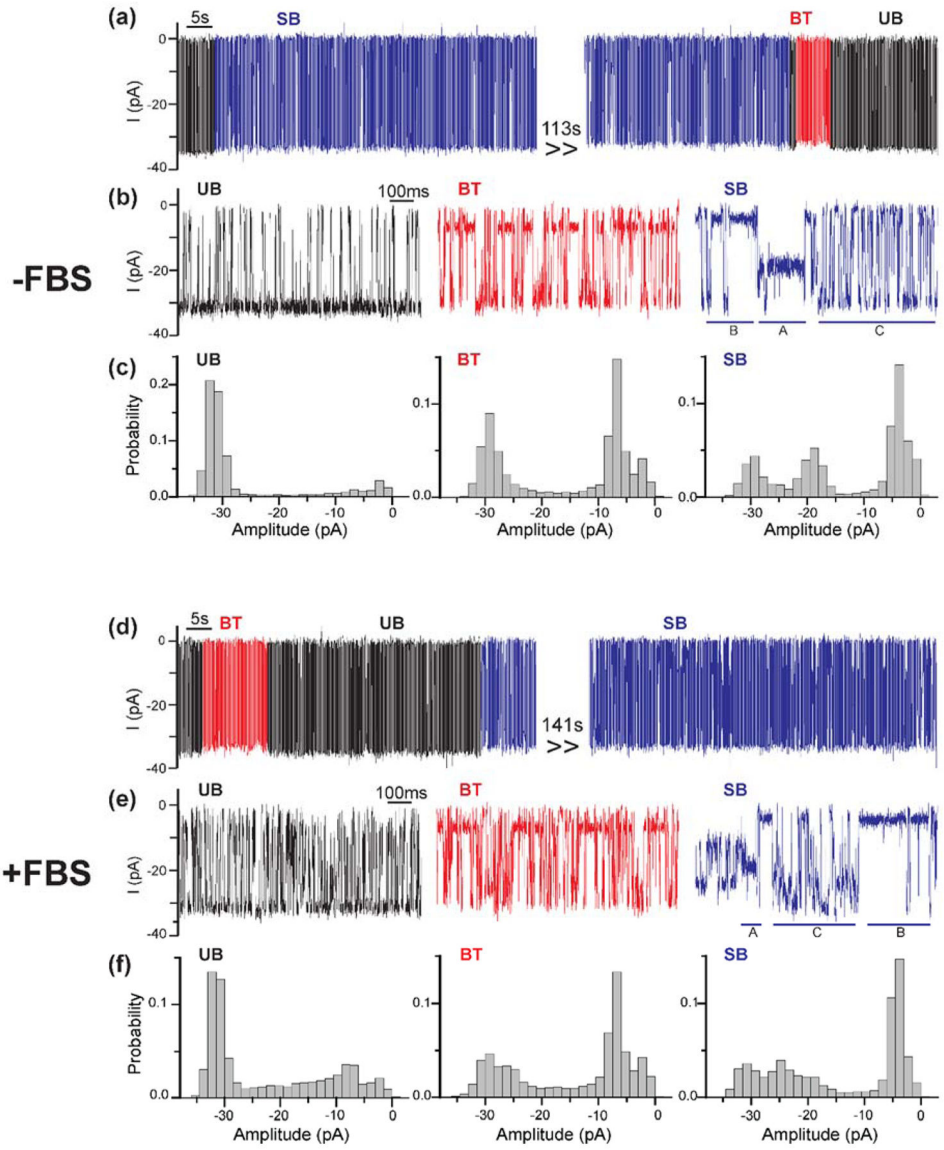

Figure 4.

Discrimination of two antibodies in the presence of serum. (a) Binding of SB (blue) and BT (red) to OmpG-biotin in the absence of serum. (b) Electrophysiology traces and (c) histograms of the unbound state in comparison with the BT and SB bound states. Buffer used was 10 mM sodium phosphate pH 6.0, 300 mM KCl and recorded at −50 mV. SB (1 nM) and BT (5 nM) were added to the recording chamber. (d) BT and SB binding in the presence of serum. (e) Electrophysiology traces and (f) histograms of BT and SB binding in the presence of serum. In addition to SB and BT, serum (10% v/v) was added to the loop-containing chamber. SB and BT binding were recorded with a 2 kHz Bessel filter at a sampling rate of 100 μs.

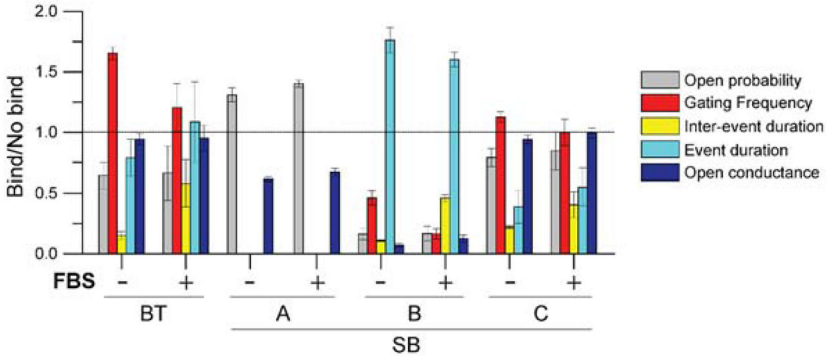

Figure 5.

The effect of serum on the fingerprint pattern of BT and SB. The gating events of different analyte protein binding states were characterized by five parameters, i.e. open probability, gating frequency, inter-event duration, event duration and the conductance of the open pore state. Changes of these parameters relative to the no binding state generate the fingerprint unique for each antibody. For SB, the three types of gating pattern were analyzed separately. The error bars indicate standard deviations from at least three independent pores.